# Electronic Supplementary Information (ESI)

## Facile Synthesis of Highly Active and Stable Pt−Ir/C Electrocatalysts for Oxygen Reduction and Liquid Fuel Oxidation Reaction

Seung Jun Hwang[a], Sung Jong Yoo[a], Tae-Yeol Jeon[b], Kug-Seung Lee[a], Yung-Eun Sung[b], Tae-Hoon Lim[a], and Soo-Kil Kim[a]*

[a] *Fuel Cell Center, Korea Institute of Science and Technology (KIST), Seoul, 136-791, Republic of Korea,*

[b] *School of Chemical and Biological Engineering, Seoul National University, Shinlimdong 56-1, Seoul, 151-742, Republic of Korea.*

*E-mail: sookilkim@kist.re.kr*

**Experimental details**

# Experimental details

## Synthesis of carbon-supported Pt−Ir catalysts (30 wt % of $Pt_1Ir_1$/C)

Carbon-supported Pt−Ir alloy nanoparticles were synthesized via conventional sodium borohydride reduction in anhydrous ethanol at room temperature. All chemicals were purchased from Aldrich with the exception of cetyltrimethylammonium bromide (CTAB, TCI) and were of analytical grade. Unless otherwise stated, all commercial reagents and solvents were used without additional purification. Pt and Pt−Ir alloy nanoparticles were prepared as follows:

To a three-neck round bottle flask (250 mL), cetyltrimethylammonium bromide (1.17g, 3.38 mmol, 10 equiv of metal precursor) was added to anhydrous ethanol (120 mL), and carbon black (Vulcan XC-72R, 0.15g) was then dispersed in the solution. After stirring for additional 30 min, $PtCl_4$ (53 mg, 0.16 mmol) and $IrCl_3$ (47 mg, 0.16 mmol) dissolved in anhydrous ethanol (50 mL) were added to the reaction mixture, and then stirred for 4 h at room temperature under Ar atmosphere. $NaBH_4$ (152 mg, 4 mmol) dissolved in 20 mL of anhydrous ethanol was quickly added to a reaction mixture and vigorous stirring for 4 h. To an obtained crude mixture was then filtered, washing with pure ethanol (J.T. Baker 99.0 %), and dried in the vacuum oven at 40 $^oC$ for 4 h. In order to get rid of surfactant from the surface of Pt−Ir alloy nanoparticles, heat treatment of as-prepared alloy electrocatalysts was performed at 250 $^oC$ under mixed gas (Ar + 5 vol % $H_2$) for 2 h. Carbon supported pure Pt, Ir, and Pt−Ir alloy nanoparticles with different composition ($Pt_3Ir_1$/C and $Pt_1Ir_3$/C) were prepared by the same method as described above, except for the amounts of metal precursor added.

## Characterization

Prepared Pt−Ir electrocatalysts were examined by X-ray diffraction (XRD, Rigaku D/Max 2500) with Cu Kα radiation, and X-ray photoelectron spectra (XPS, PHI 5800 ESCA) were obtained from a monochromator (Al Kα source) calibrated with respect to the C (1s) peak at 284.6 eV. EXAFS was conducted at the Pohang Light Source (PLS) with a ring current of 120–170 mA at 2.5 GeV using the 5A1 beamline. Particle size, size distribution, dispersion were confirmed by transmission electron microscopy (TEM, Philips CM30) and high resolution transmission electron microscopy (HR-TEM, FEI, 200 keV). The composition of prepared Pt−Ir alloy nanoparticles were analyzed by inductively coupled plasma (ICP, Elan 6100 DRC plus, Perkin-Elmer). Optimum heat treatment condition for removing unwanted surfactants was evaluated by temperature programmed reduction (TPR, BELCAT M-125, BEL Japan, Inc.) and thermogravimetric analysis (TGA, Ta Instrument, Inc.).

## Electrochemical measurement

Cyclic voltammetry (CV) and linear sweep volatammetry (LSV) were performed using an Autolab PGSTAT20 potentiostat and a rotating disk electrode (RDE) system (Pine) in a standard three-electrode configuration. An alloy-deposited glassy carbon electrode with a diameter of 5 mm was used as the working electrode and a platinum wire was used as the counter electrode. All electrochemical measurements were performed in Ar-purged 0.1 M $HClO_4$ or 0.5 M $H_2SO_4$ solution except for the ORR (purged for 30 min in $O_2$), and the cell temperature was fixed at 298 K.

The catalyst ink was prepared by mixing 10 mg of carbon supported nanoparticles with 50 μL of DI water, 100 μL of nafion as a binder material, and 1mL of isopropyl alcohol. Follow mixing and ultrasonification, 7μL of ink slurry was pipetted onto a glassy carbon substrate. The dried electrode was then transferred to the electrochemical cell for electrochemical measurements. CV measurements were recorded between 0.05 V and 0.8 V with respect to normal hydrogen electrode (NHE) at a scan rate of 20 mV/s in Ar purged 0.5 M $H_2SO_4$ solution. The activity of liquid fuel oxidations were measured in an Ar-purged 0.5 M $H_2SO_4$ and 1 M of liquid fuel solution (ethanol, methanol, and formic acid) with the scan rate of 20 mV/s between 0.05 and 1.20 V with respect to NHE. ORR polarization curves were initially recorded at 298 K in an $O_2$ saturated 0.1 M $HClO_4$ solution with a sweep rate of 5 mV/s and a rotation rate of 1600 rpm (from 0.05 to 1.05 V with respect to RHE). For the stability test, accelerated cycling was conducted between 0.05 and 0.95 V with 50 mV/s. After 3000 and 10000 cycle, ORR polarization curves were again recorded with the same condition to compare its activity difference.

# Supporting Information Figure Caption

S1. TEM images of $Pt_1Ir_1$ electrocatalysts prepared with various solvents.

S2. TEM images of $Pt_1Ir_1$ electrocatalysts prepared by using cationic surrfactants with different alkyl chain length.

S3. 10 mg of as-prepared $Pt_1Ir_3$ catalysts were subjected to temperature programmed reduction (TPR) analysis at 5 % $H_2$ / 95 % Ar gas flow atmosphere with the ramping temperature of $5^oC$ / min.

S4. 10 mg of as-prepared $Pt_1Ir_3$ (a) and heat-treated $Pt_1Ir_3$ (b) catalysts were conducted thermogravimetric analysis (TGA) at air atmosphere with the ramping temperature of $5^oC$ / min.

S5. (a) Deviation of size distribution of as-prepared $Pt_1Ir_1$ under different pH condition. (b) X-ray diffraction data of as-prepared $Pt_1Ir_1$ catalysts generated from different pH solution.

S6. TEM images, diffraction patterns, and EDX datas of heat-treated 30 wt % Pt/C, $Pt_3Ir_1$/C, $Pt_1Ir_1$/C, $Pt_1Ir_3$/C, Ir/C.

S7. Percentage of degree of alloying of prepared Pt−Ir alloy catalysts based on Vegards law.

S8. Pt 4f XPS fitting data of heat-treated electrocatalysts: (a) Pt/C, (b) $Pt_3Ir_1$/C, (c) $Pt_1Ir_1$/C, (d) $Pt_1Ir_3$/C, and (e) Pt (0) binding energy as a function of degree of alloying.

S9. Ir 4f XPS fitting data of heat-treated electrocatalysts: (a) Ir/C, (b) $Pt_1Ir_3$/C, (c) $Pt_1Ir_1$/C, (d) $Pt_3Ir_1$/C, and (e) Ir (0) binding energy as a function of degree of alloying.

S10. (a) the ratio of Pt states (Pt(0), Pt(II), Pt(IV) for each compositions and (b) Ir ratio in the same way.

S11. Energy edge difference of Pt and Ir: Pt $L_{III}$, Pt $L_{II}$, Pt $L_I$, Ir $L_{III}$, Ir $L_{II}$, and Ir $L_1$.

S13. The color of (a) Ir precursor, and cetyltrimethylammonium bromide (CTAB) in 120 mL EtOH, (b) Ir precursor in 120 mL EtOH.

## S1. Solvent effect

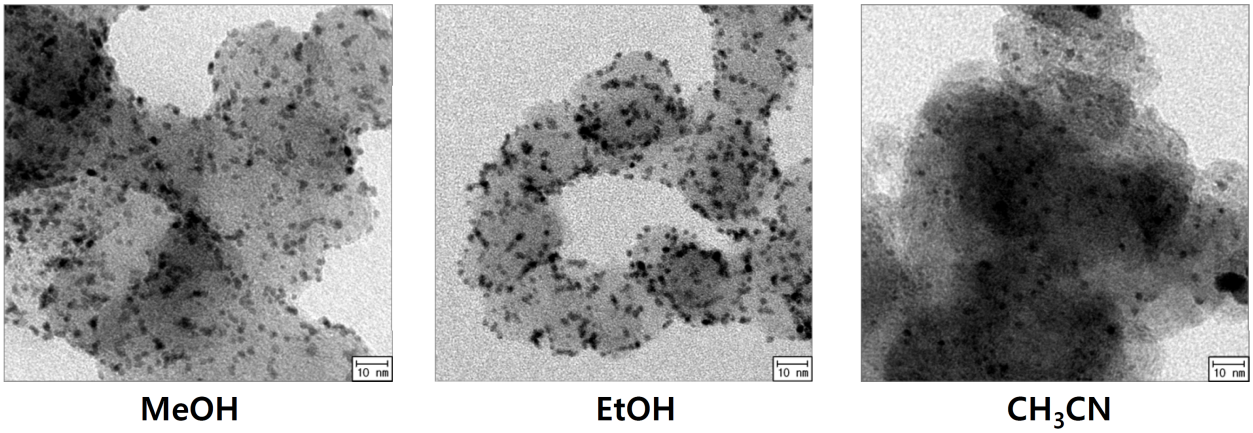


## S2. Alky chain effect

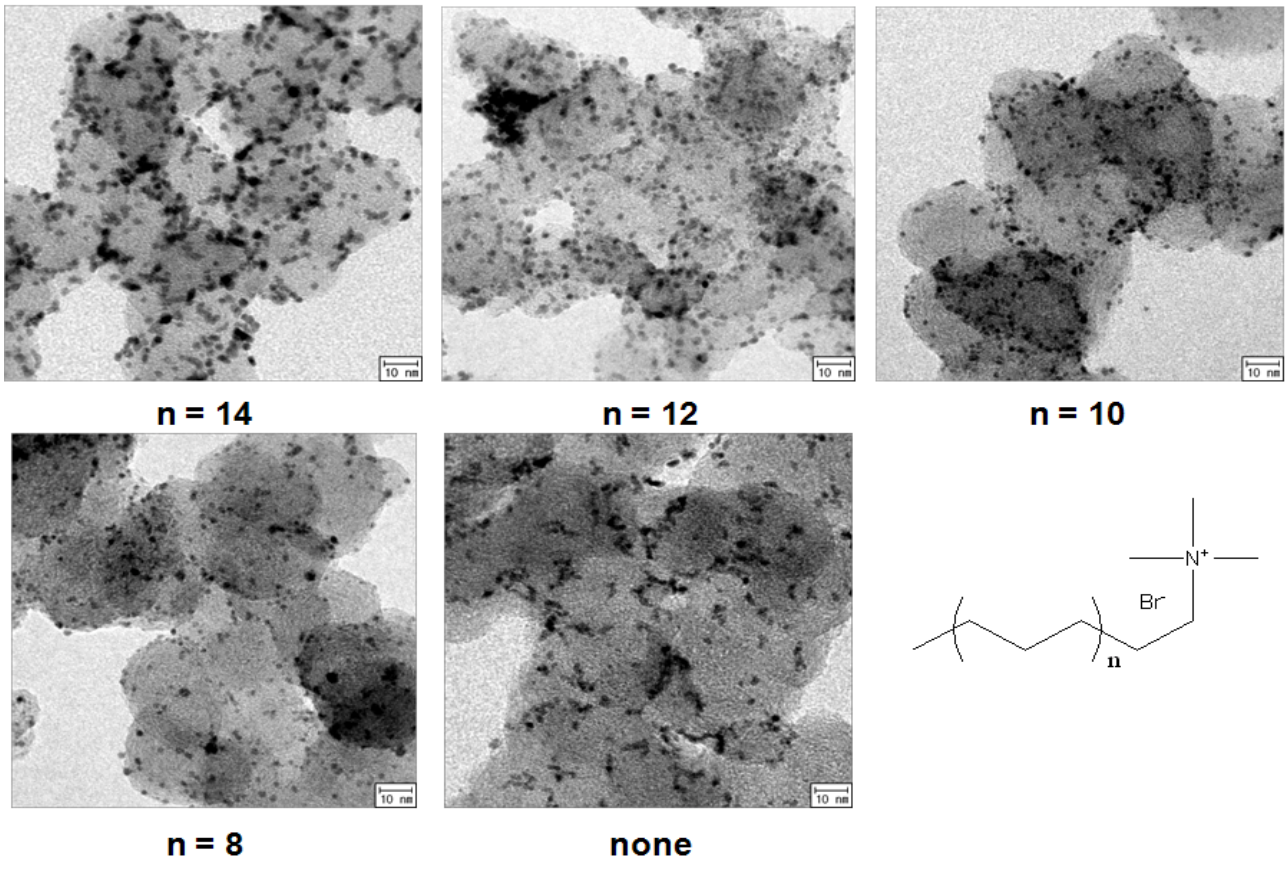

## S3. TPR data

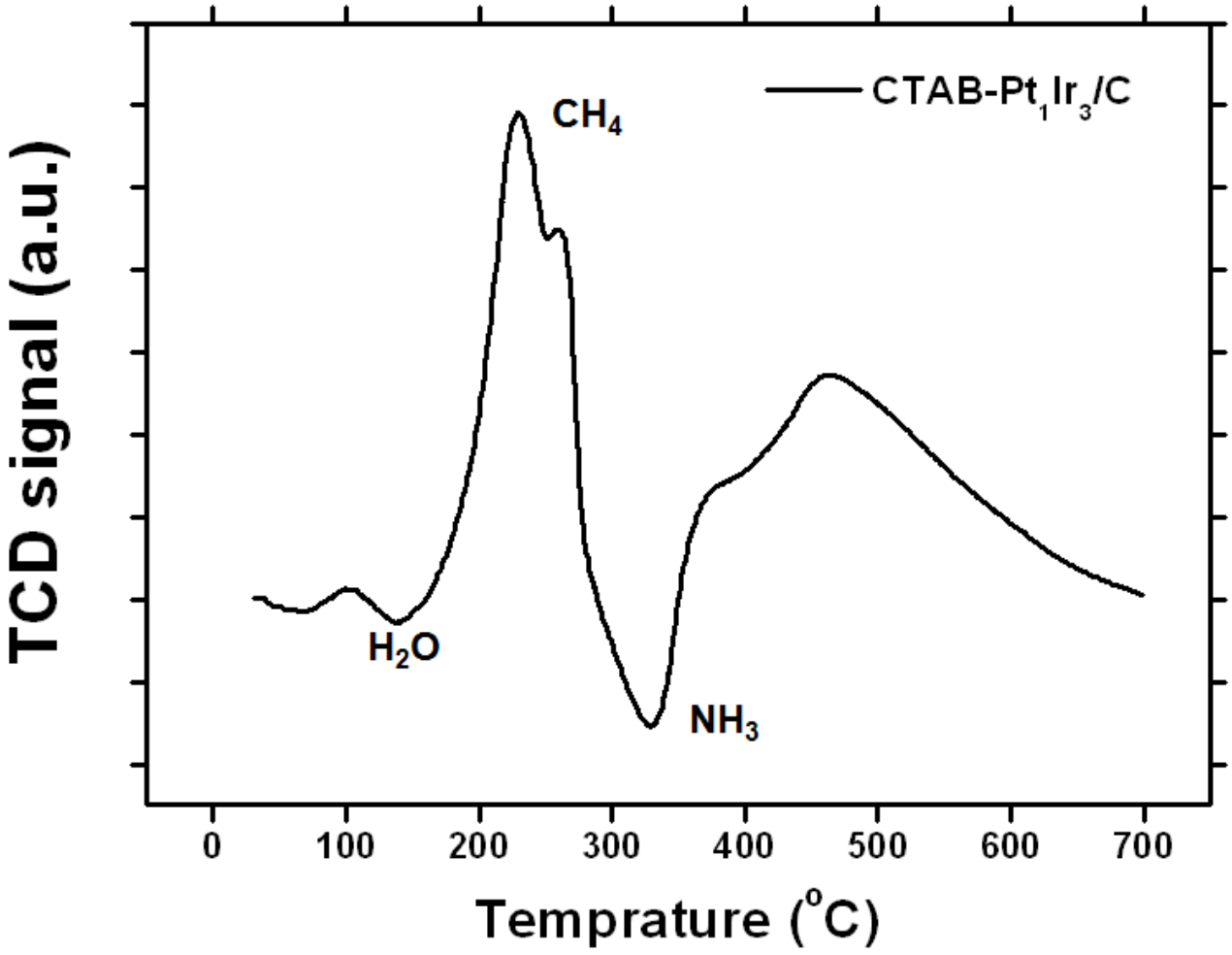


| Name of gas | Thermal conductivity ($10^{-4}$ W/m K) |
|---|---|
| $H_2$ | 1815 |
| Ar | 178.7 |
| $H_2O$ | 181 |
| $CH_4$ | 343 |
| $NH_3$ | 246 |
| Flow gas | 260.5 |

# S4. TGA data

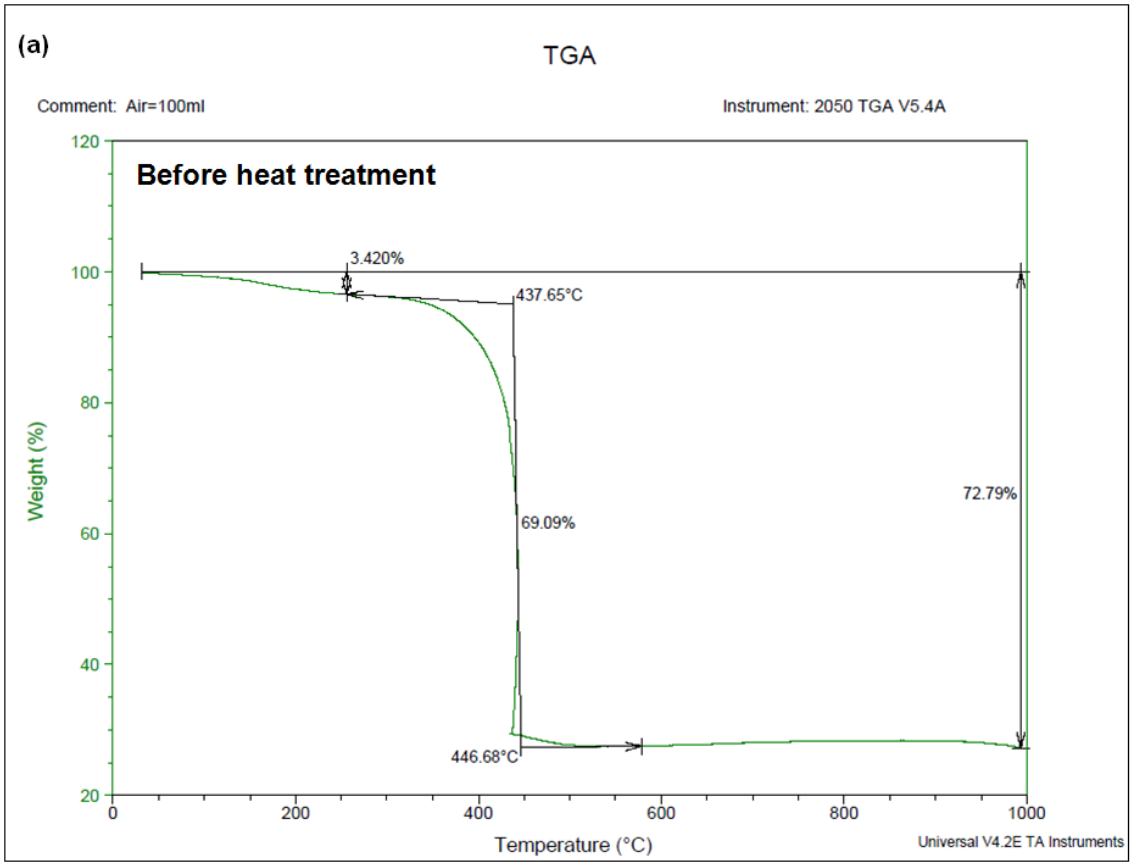
(a)
TGA
Comment: Air=100ml
Instrument: 2050 TGA V5.4A
Before heat treatment
3.420%
437.65°C
69.09%
72.79%
446.68°C
Weight (%)
Temperature (°C)
Universal V4.2E TA Instruments

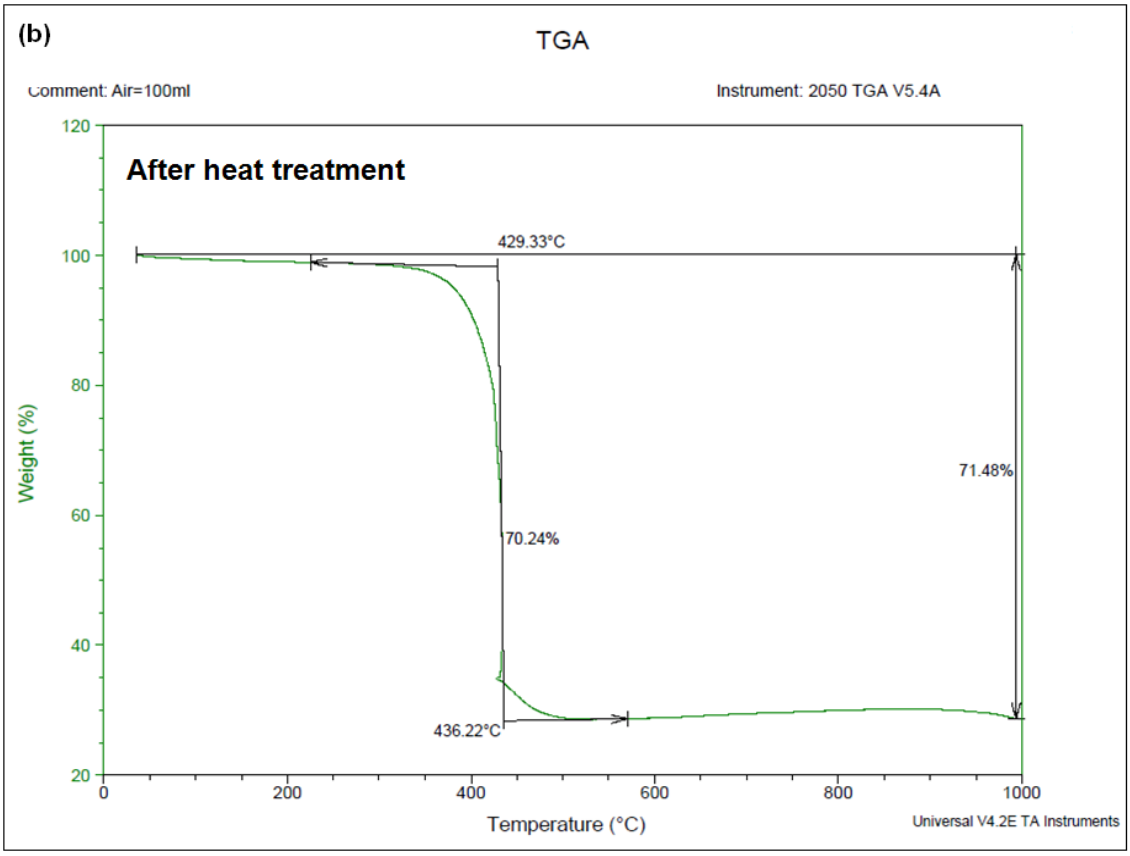
(b)
TGA
Comment: Air=100ml
Instrument: 2050 TGA V5.4A
After heat treatment
429.33°C
70.24%
71.48%
436.22°C
Weight (%)
Temperature (°C)
Universal V4.2E TA Instruments

## S5. pH effect

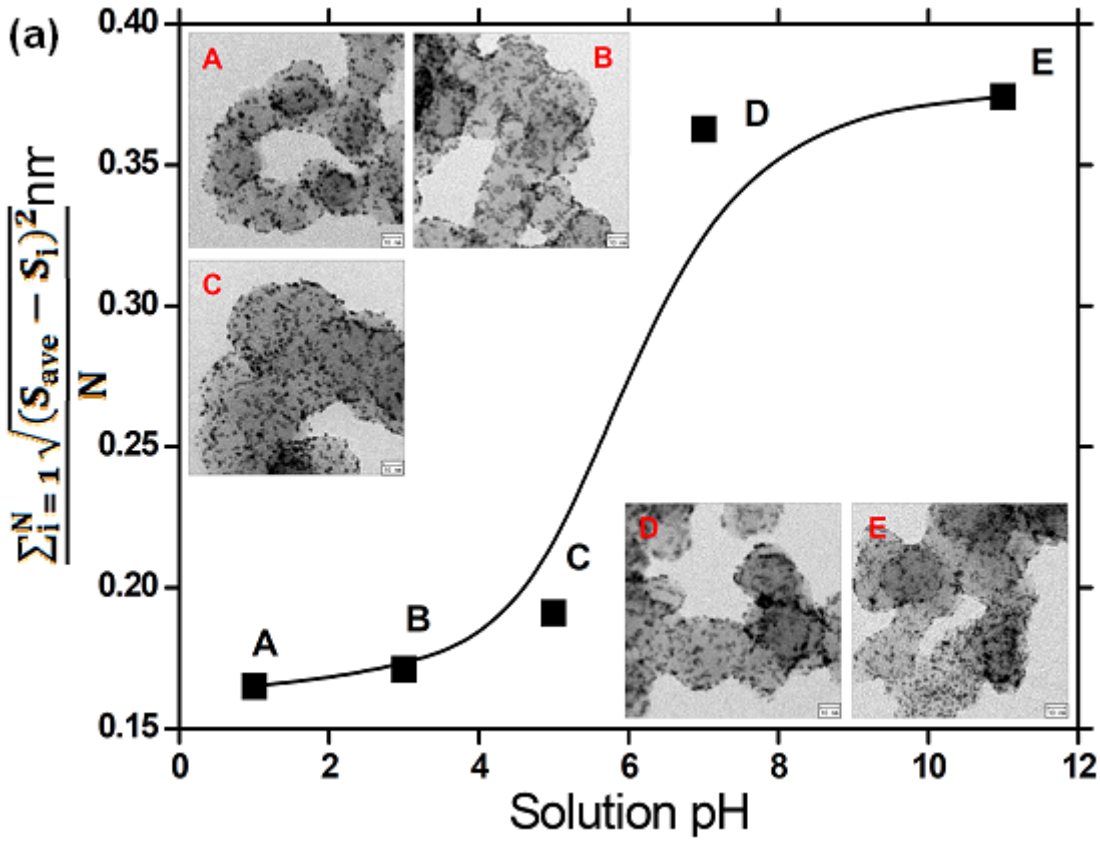
(a)
$\frac{\sum_{i=1}^{N}\sqrt{(S_{ave}-S_i)^2}nn}{N}$
0.40
0.35
0.30
0.25
0.20
0.15
0
2
4
6
8
10
12
Solution pH
A
B
C
D
E

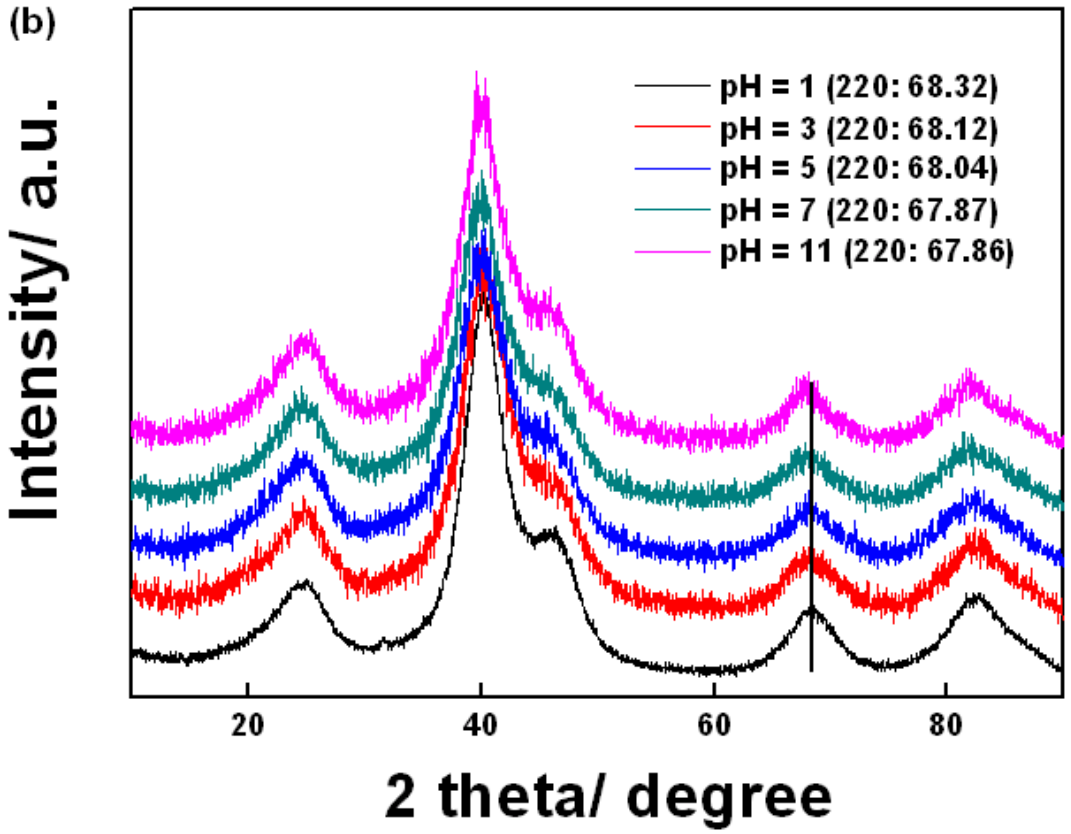
(b)
Intensity/ a.u.
pH = 1 (220: 68.32)
pH = 3 (220: 68.12)
pH = 5 (220: 68.04)
pH = 7 (220: 67.87)
pH = 11 (220: 67.86)
20
40
60
80
2 theta/ degree

# S6: TEM images (After heat treatment)

## 1) 30 wt % Pt/C

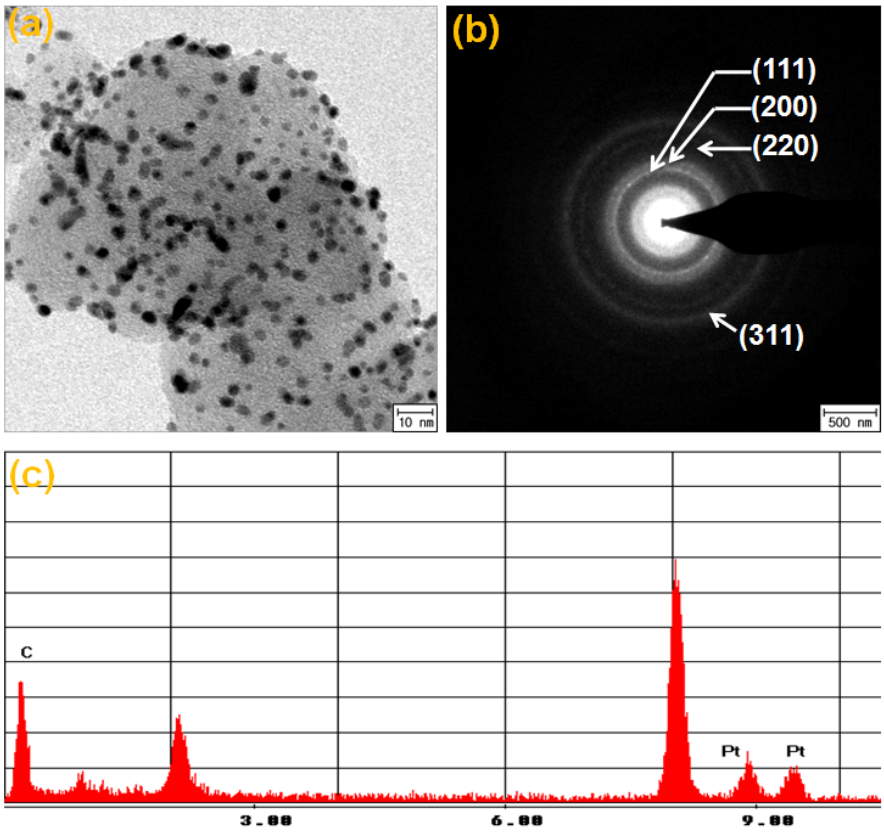


## 2) 30 wt % $Pt_3Ir_1$/C

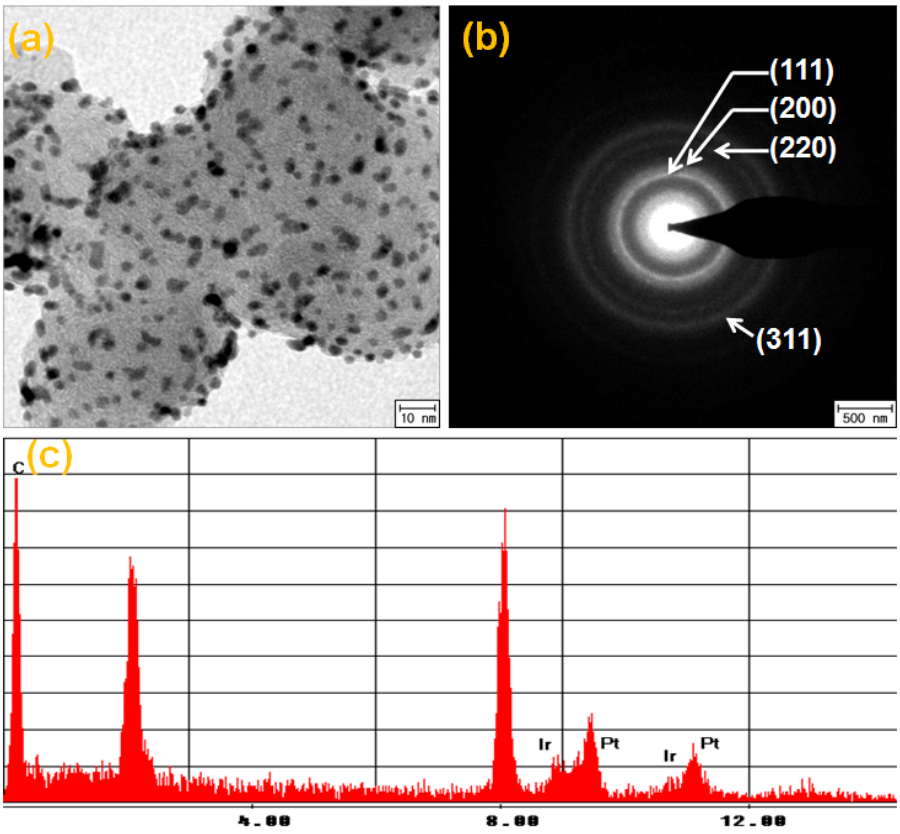

## 3) 30 wt % $Pt_1Ir_1/C$

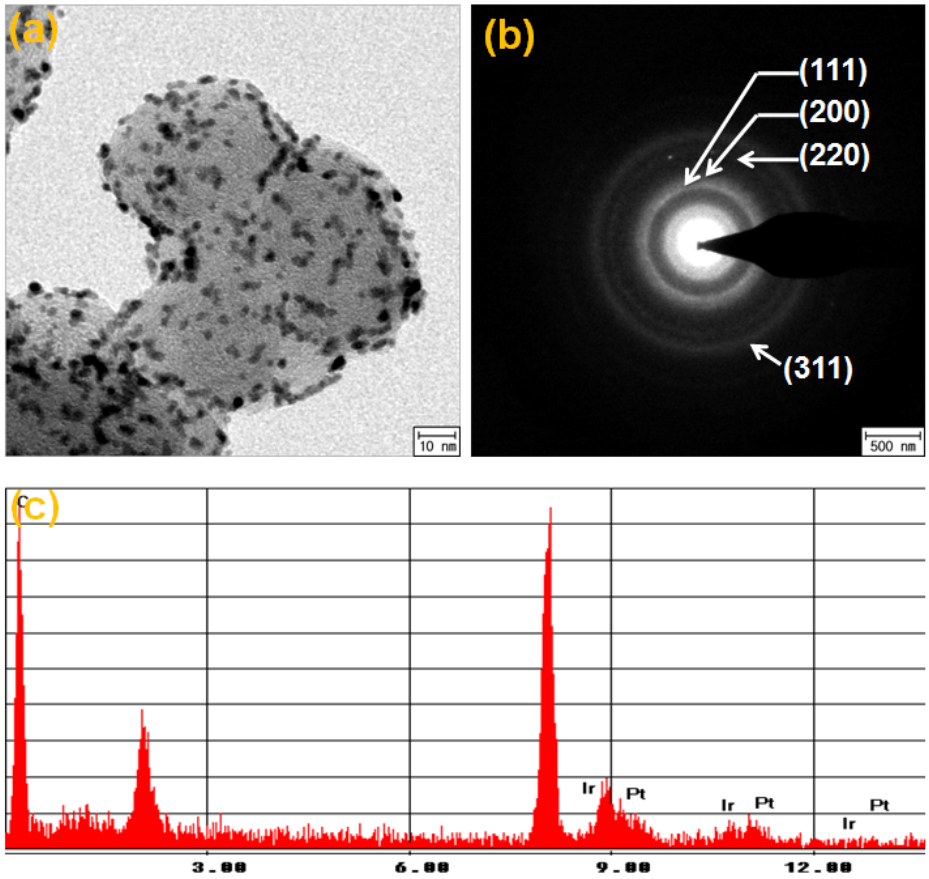


## 4) 30 wt % $Pt_1Ir_3/C$

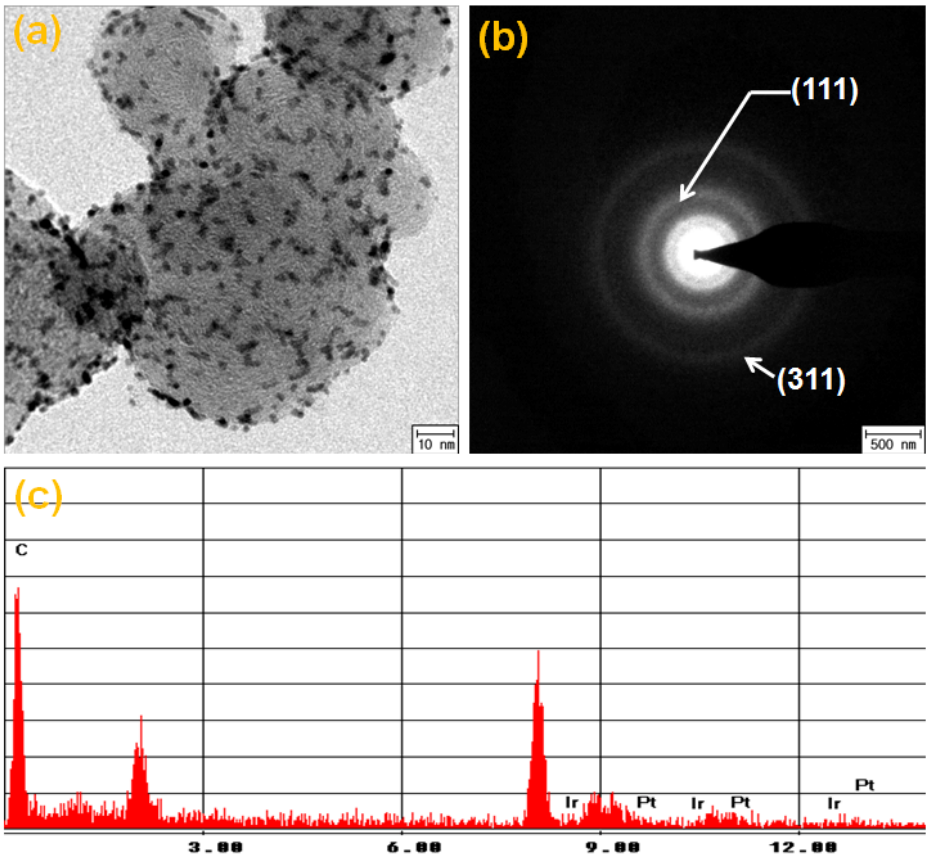

## 5) 30 wt % Ir/C

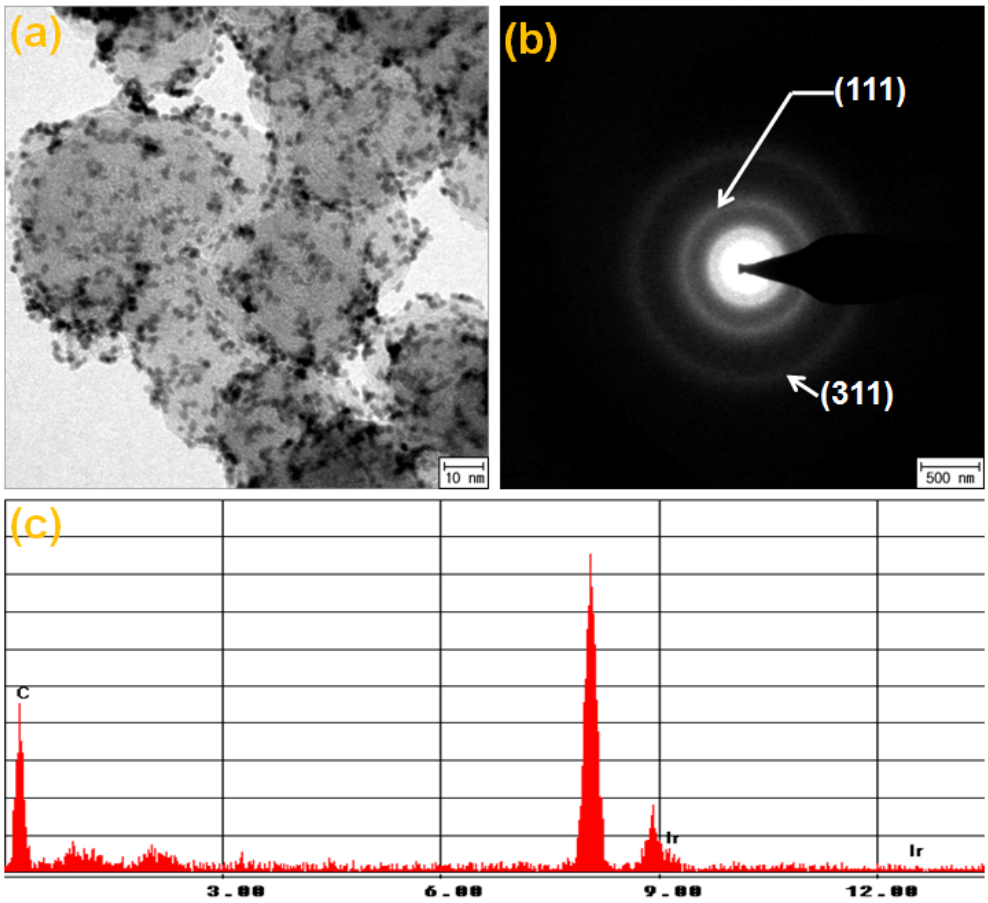


## S7. Vegard's law

| | Exp | Vegard | Degree of Alloying (%) |
|---|---|---|---|
| Pt | 3.91 | 3.92 | 99.7 |
| $Pt_3Ir_1$ | 3.90 | 3.90 | 100 |
| $Pt_1Ir_1$ | 3.88 | 3.88 | 100 |
| $Pt_1Ir_3$ | 3.86 | 3.86 | 100 |
| Ir | 3.84 | 3.84 | 100 |

# S8. XPS data fitting: Pt

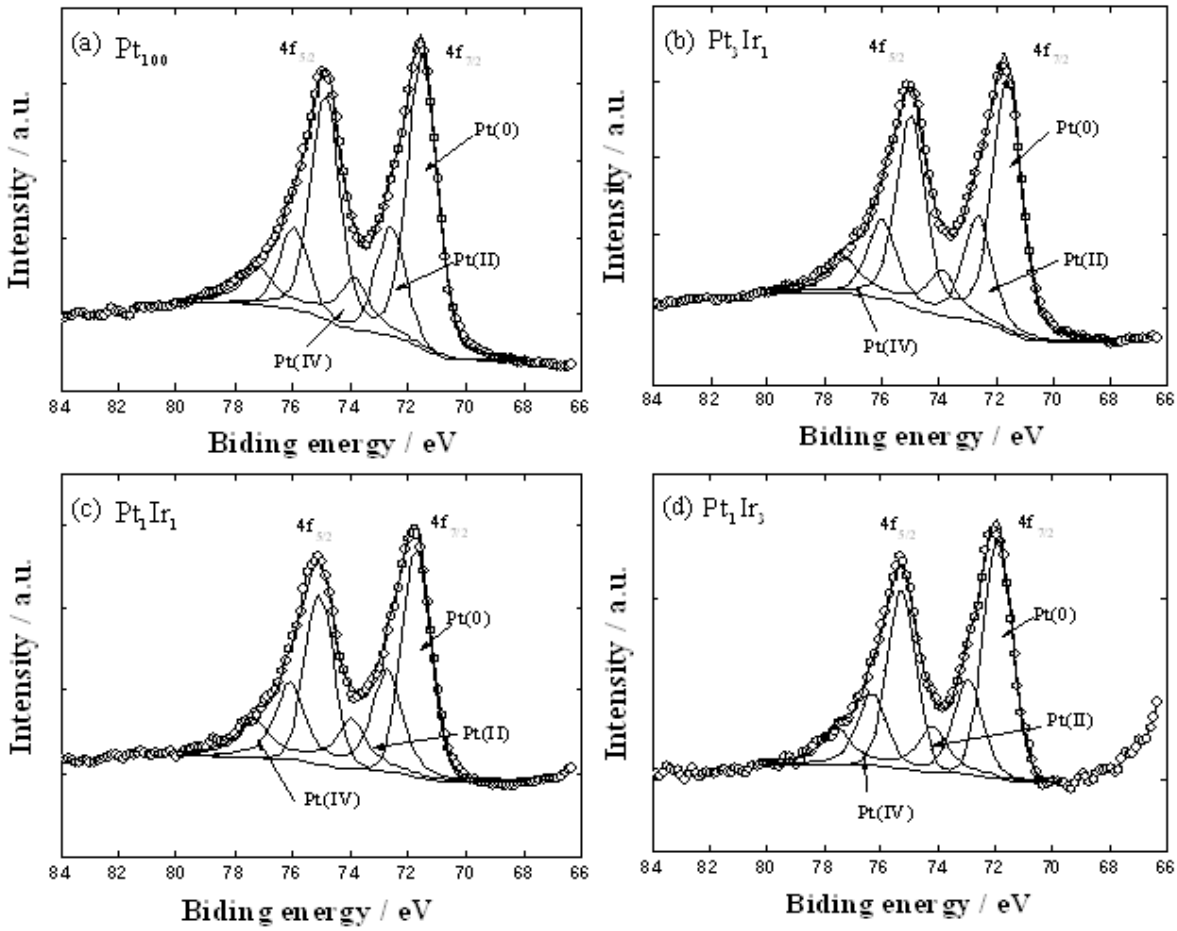


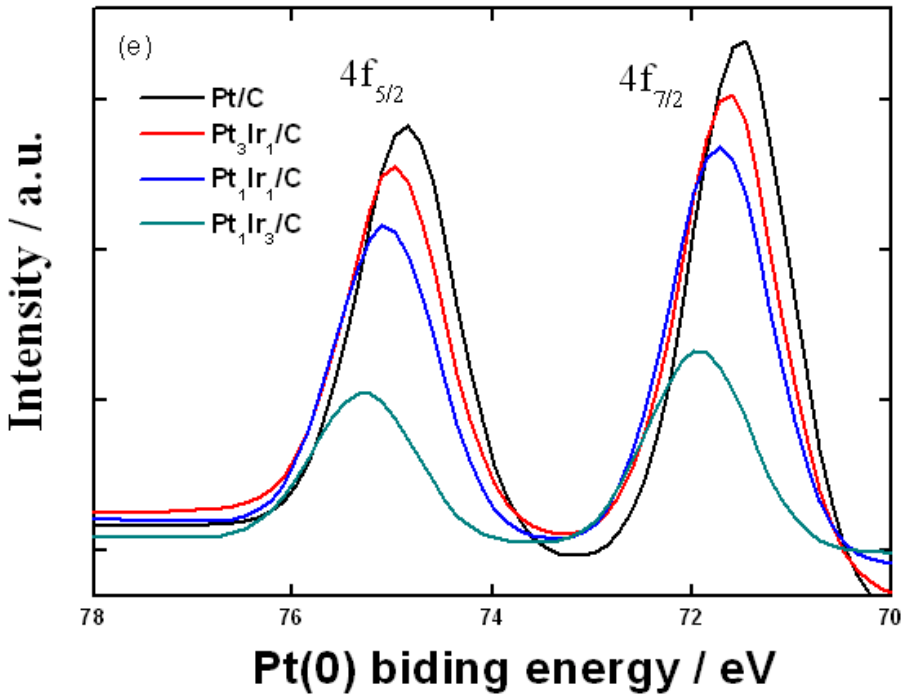

# S9. XPS data fitting: Ir

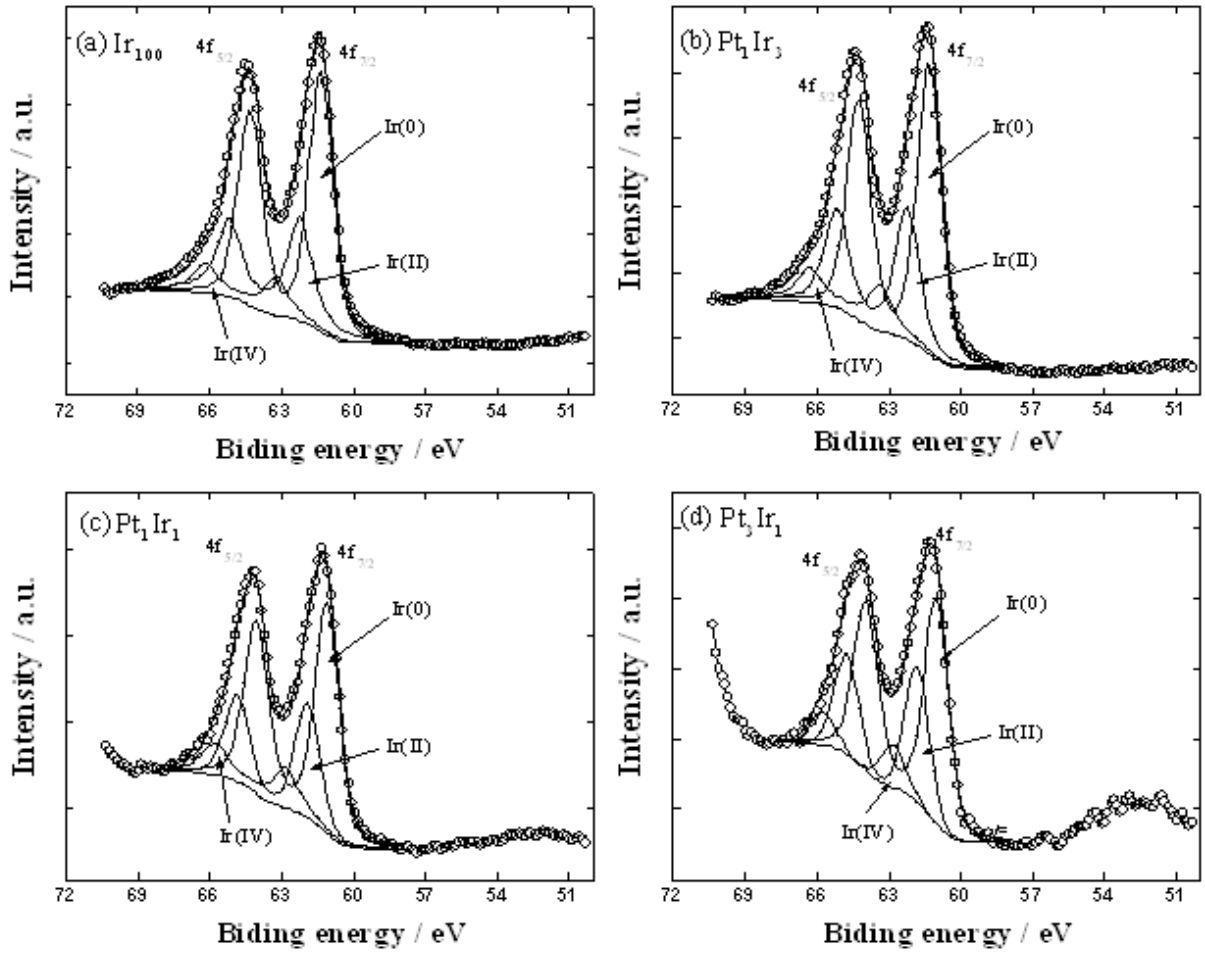


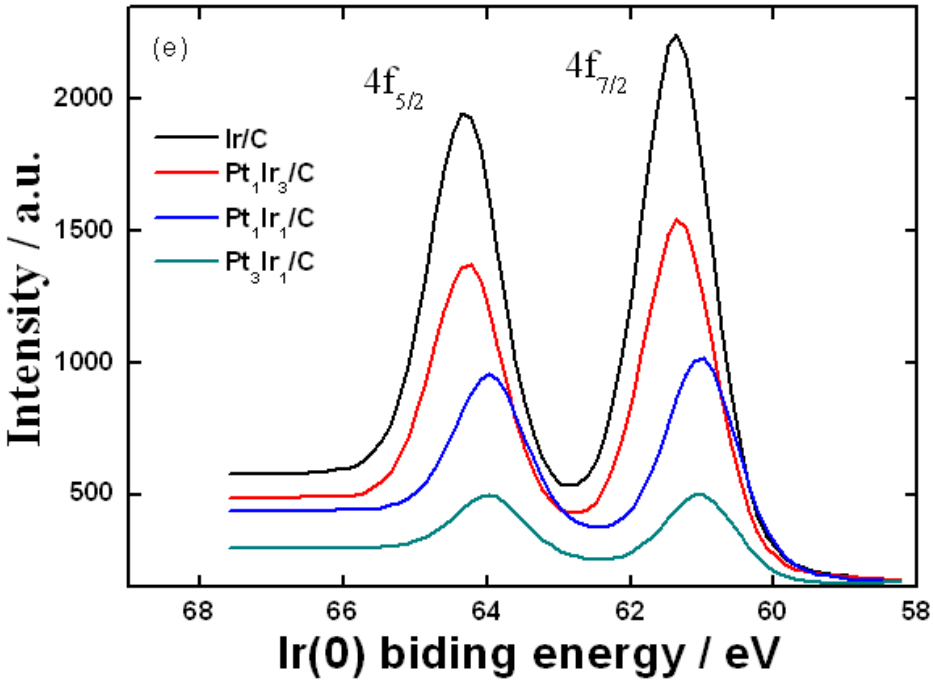

## S10. Pt, Pt(II), Pt(IV) ratio / Ir, Ir(II), Ir(IV) ratio

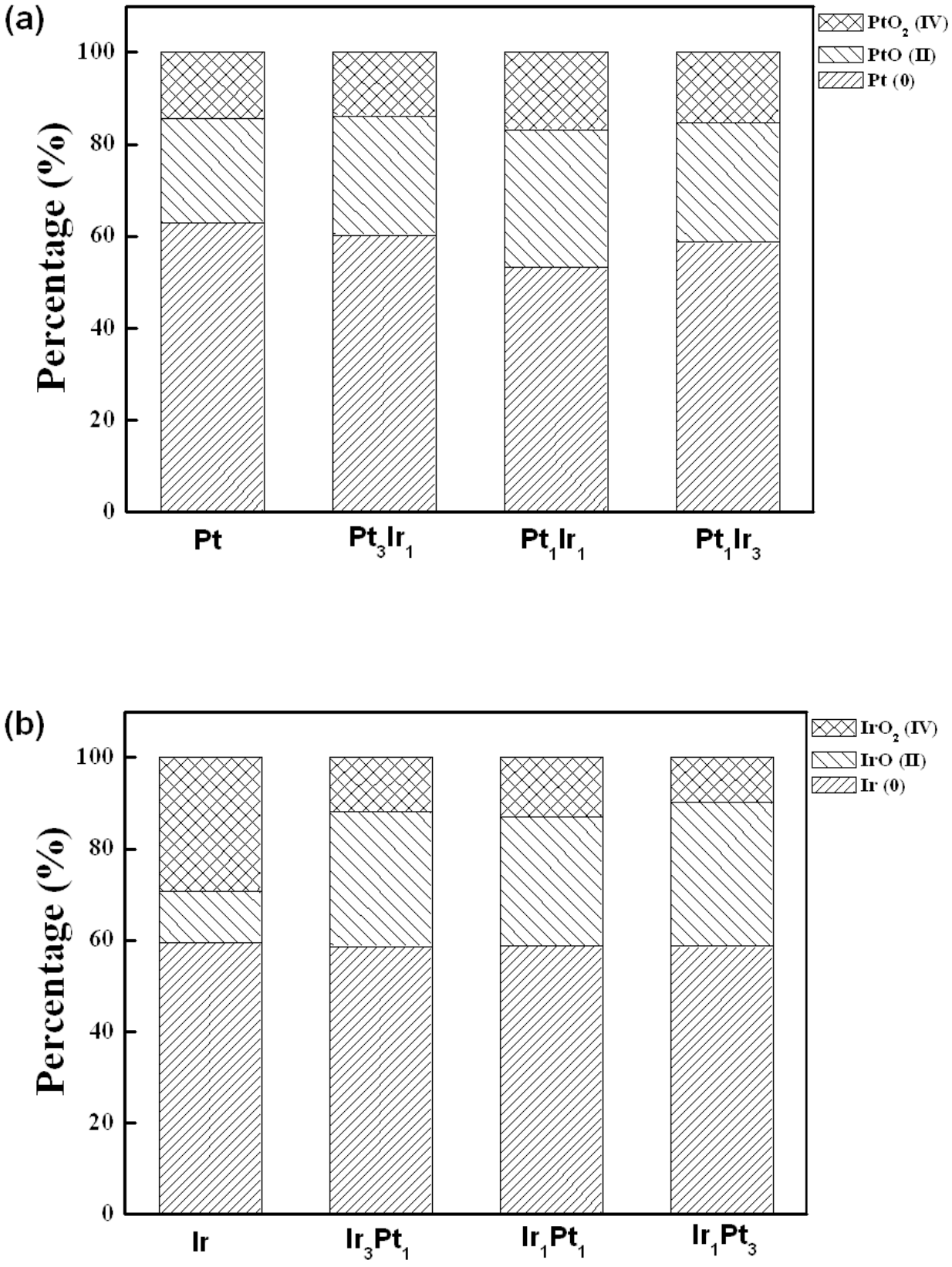

## S11. EXAFS edge measured

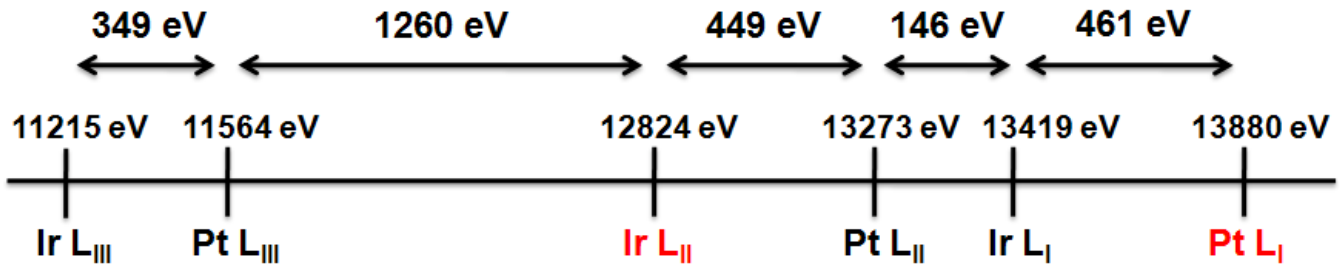


## S12. Synchrotron X-ray absorption fine structure (XAFS)

X-ray absorption fine structure (XAFS) experiments were conducted on 5A beamline of Pohang Accelerator Laboratory (PAL) (2.5 GeV; 150-180 mA). The incident beam was monochromatized using a Si(111) double crystal monochromator and detuned by 30 % to minimize the contamination from higher harmonics, in particular, the third order reflection of the silicon crystals. The spectra for $L_I$-edge of Pt ($E_0$ =13880 eV) were taken in a transmission mode with separate He-filled IC Spec ionization chambers for incident and transmitted beams, respectively. Before measuring samples, energy was calibrated by using of Pt foil. The energy scan was performed in five regions for good energy resolution in a steep absorption and measurement of XANES and EXAFS spectra at a time, 5 eV-step in region of 13680-13830 eV, 1 eV-step in 13830-13870 eV, 0.25 eV-step in 13870-13910 eV, 0.03 *k*-step in 13910-14420 eV, and 0.04 *k*-step in 14420-114880 eV. The obtained data were processed in the usual way to obtain the absorbance and analyzed with ATHENA and ARTEMIS in the suite of IFEFFIT software programs. Pre-edge absorption due to the background and detector were subtracted using a linear fit to the data in the range of -200 to -60 eV relative to $E_0$. $E_0$ was defined as the first inflection point on the rising absorption edge. Each spectrum was then normalized by a constant, extrapolated value to $E_0$ of third-order polynomial fit over absorption at 150-900 eV relative to $E_0$. To isolate EXAFS signal, the post-edge background function was approximated with a piecewise spline that could be adjusted so that the low-R component of pre-Fourier transformed data were minimized. After calculation of EXAFS function χ(k), $k^3$-weighted EXAFS function in momentum ($k$) space was Fourier transformed to reveal the neighboring atoms arranged according to distance from a central As atom in R-space. The k range of the transform varied between a $k_{min}$ of 2.0-3.0 Å -1 and a $k_{max}$ of 12.0-13.0 $Å^{-1}$. Kaiser-Bessel function was adopted as a window function and the windowsill of $dk$=1.5 was also used in the transform. A shell of interest in R-space was back-transformed into the momentum space with Kaiser-Bessel window functionand windowsill of $dR$=0.1. Fourier-filtered spectra derived from the experiments were fitted by using of the theoretical standards generated with the ab-initio FEFF 6 code. The standard Pt-O and Pt-Pt phase-shift and amplitude functions were extracted from the structures of β-$PtO_2$[1] and Pt metal[2], respectively. The

standard Pt-Ir functions were produced by using of the structure of Pt metal with Ir atoms replaced at the nearest neighboring Pt positions. Table 1 shows EXAFS parameters extracted from $k^3$-weighted Pt $L_I$ spectra of Pt/C and PtIr nanoparticles supported on carbon black.

**Table.** Results of model fitting of $k^3$-weighted and Fourier-filtered Pt $L_I$ EXAFS for PtIr/C.

| sample | Bond | *N* | R (Å) | $\sigma^2$ | $R_{factor}$ (%) |
|---|---|---|---|---|---|
| Pt/C (J.M.) | Pt–O | 0.96 | 1.966 | 0.0033 | 3.6 |
| | Pt–Ir | N/A | N/A | N/A | |
| | Pt–Pt | 6.60 | 2.766 | 0.0044 | |
| $Pt_1Ir_3$ | Pt–O | 1.70 | 1.95 | 0.0033* | 7.2 |
| | Pt–Ir | 1.67 | 2.57 | 0.0022 | |
| | Pt–Pt | 4.17 | 2.75 | 0.0022 | |
| $Pt_1Ir_1$ | Pt–O | 1.24 | 1.96 | 0.0033* | 4.3 |
| | Pt–Ir | 1.54 | 2.66 | 0.0053 | |
| | Pt–Pt | 7.18 | 2.77 | 0.0053 | |
| $Pt_3Ir_1$ | Pt–O | 0.87 | 1.99 | 0.0033* | 2.1 |
| | Pt–Ir | 1.63 | 2.65 | 0.0029 | |
| | Pt–Pt | 7.84 | 2.79 | 0.0029 | |

1. Notation: N, coordination number; R, interatomic distance; $\sigma^2$, Debye-Waller factor; R-factor, goodness of fit which gives a sum-of-squares measure of the fractional misfit.
2. *fixed parameter.
3. The value in parenthesis denotes the estimated error of the calculated parameter.

1. Siegel, S. et al. The crystal structure of beta-platinum dioxide. J. Inorg. Nucl. Chem. 31, 3803-3807 (1969).
2. Kasper, J. S. & Lonsdale, K. International Tables for X-ray Crystallography. V.3. D. Reidel Pub. Co., 1985.

## S13. Complex Colour Change

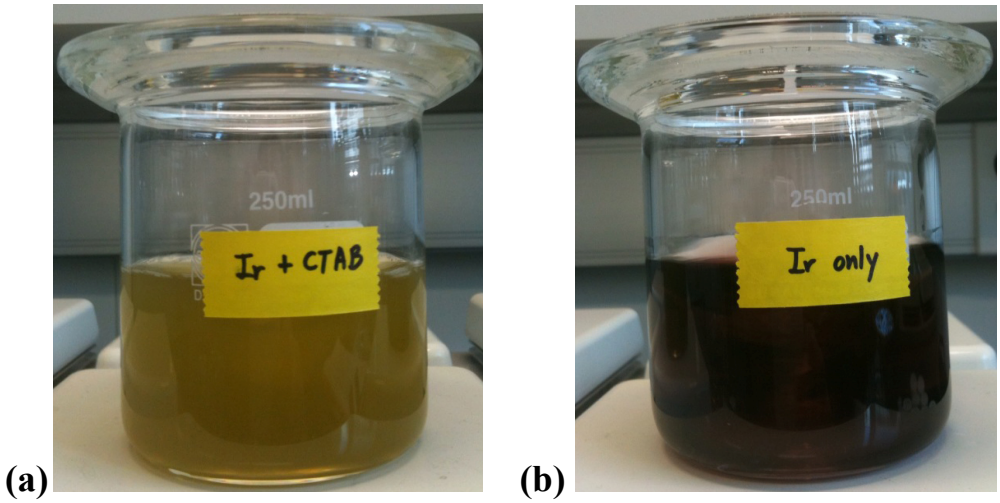

## S14. Alcohol oxidation table

| | EtOH oxidation | | | MeOH oxidation | | | HOOOH oxidation | | |
|---|---|---|---|---|---|---|---|---|---|
| | Onset potential (vs.NHE) | $I_b/I_f$ | Peak current ($mA/mg_{Pt}$) | Onset potential (vs.NHE) | $I_b/I_f$ | Peak current ($mA/mg_{Pt}$) | Onset potential (vs.NHE) | $I_b/I_f$ | Peak current ($mA/mg_{Pt}$) |
| Pt/C | 0.320 | 0.78 | 319.2 | 0.553 | 1.09 | 129.9 | 0.285 | 3.60 | 507.8 |
| $Pt_3Ir_1/C$ | 0.271 | 0.67 | 544.3 | 0.336 | 0.67 | 436.2 | 0.245 | 2.45 | 921.9 |
| $Pt_1Ir_1/C$ | 0.244 | 0.64 | 579.7 | 0.428 | 0.33 | 350.2 | 0.210 | 2.21 | 1043.7 |
| $Pt_1Ir_3/C$ | 0.232 | 0.40 | 486.2 | 0.372 | 0.07 | 371.3 | 0.105 | 1.17 | 1283.2 |

## S15. Electrochemical activity by Price

**(Pt: 51 $/g, Ir: 23 $/g, 2010. 09. 15, from Johnson Matthey)**

### 1) Ethanol oxidation

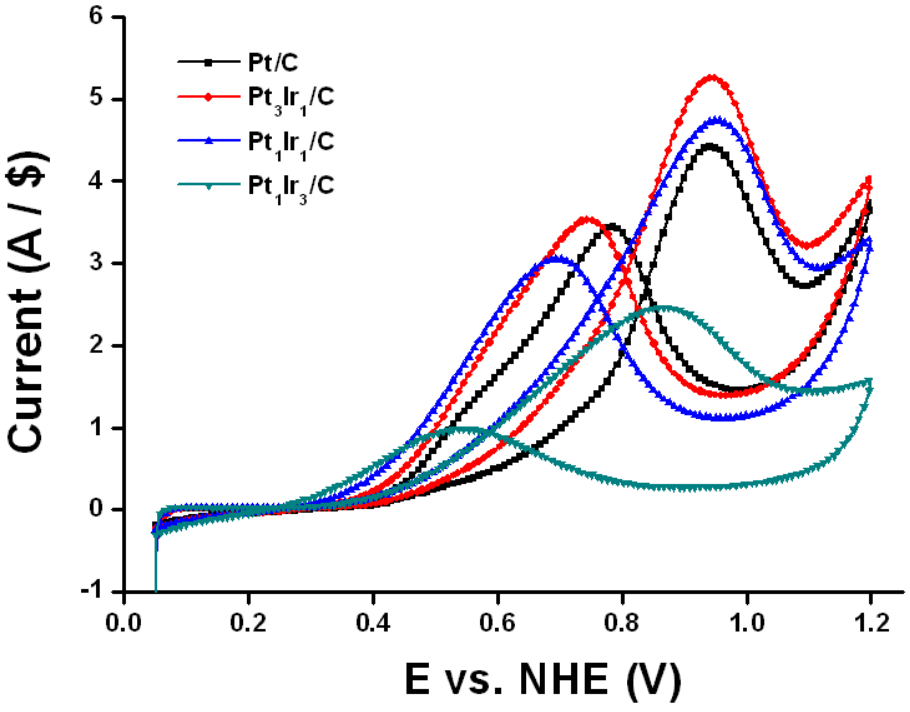

## 2) Methanol oxidation

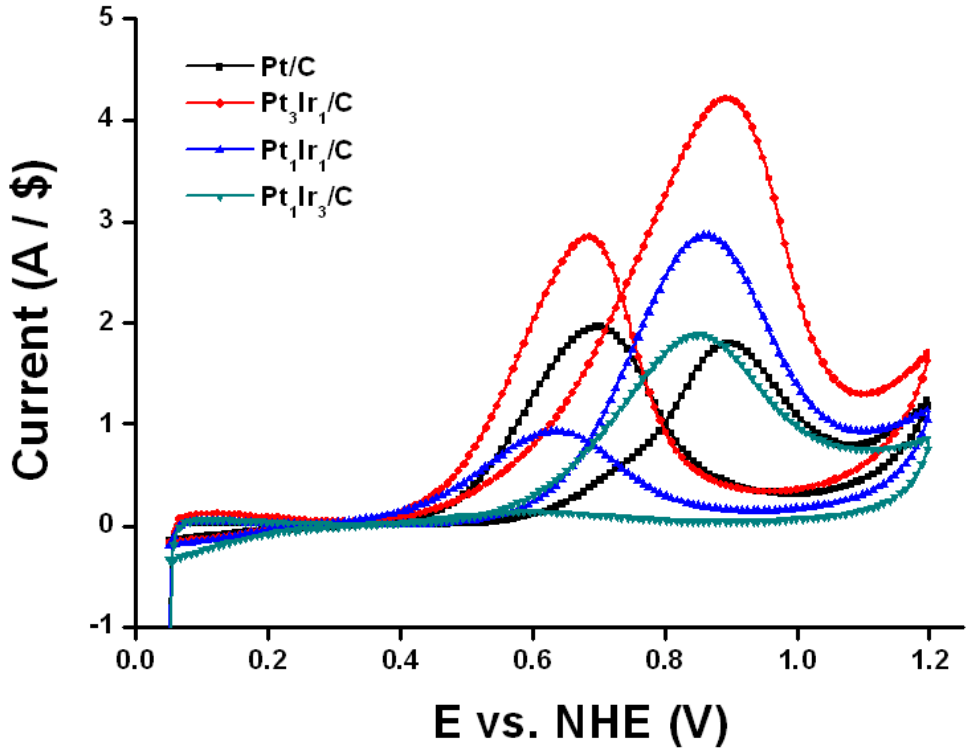


## 3) Formic acid oxidation